

Figure 3.2 Phase diagram of water.

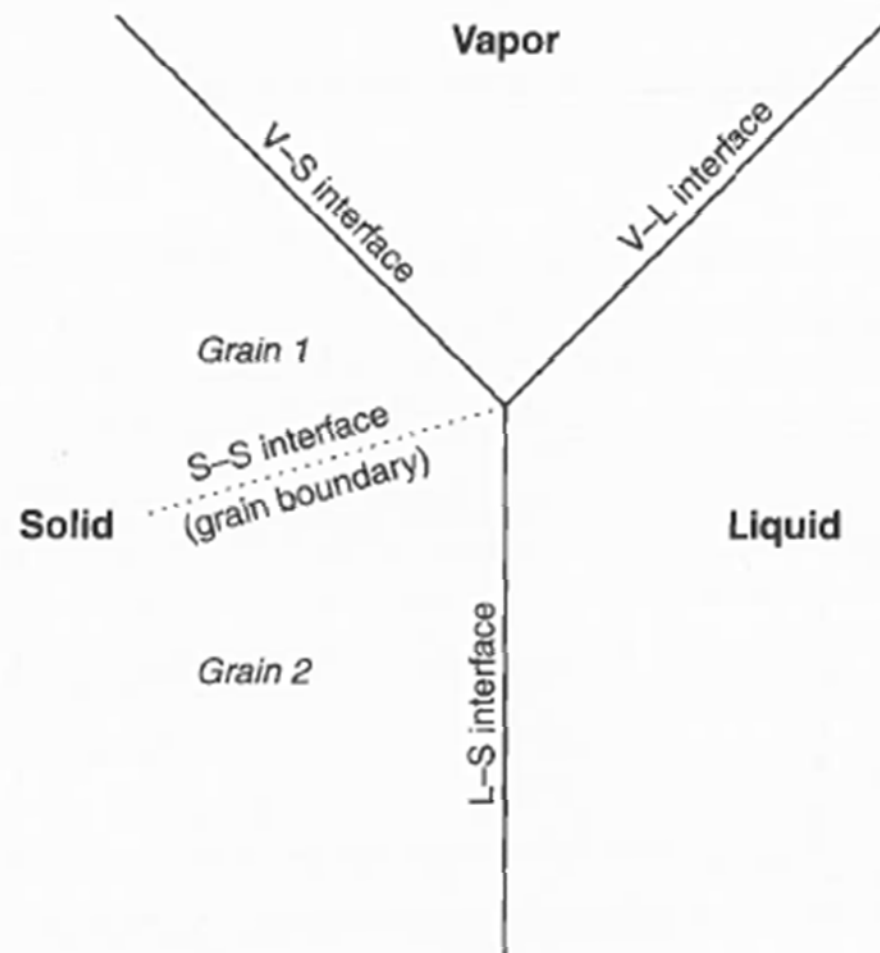


Figure 3.3 Schematic depiction of the various phases and interfaces of water.

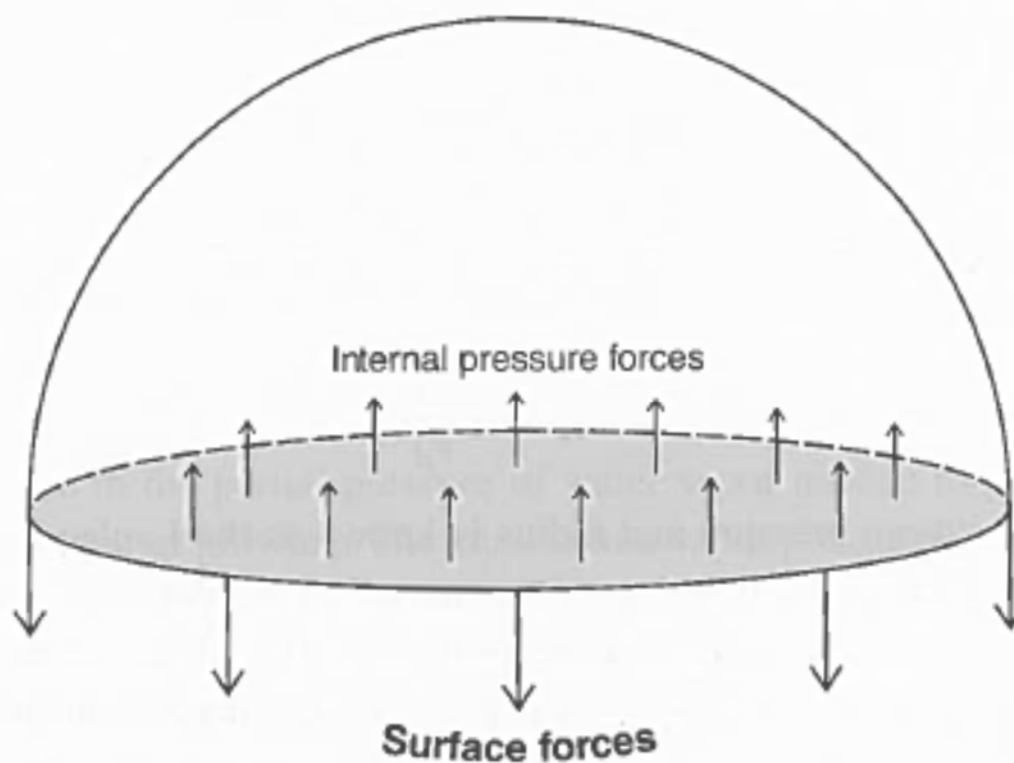


Figure 3.4 Cross section of a liquid drop showing the forces involved in maintaining mechanical equilibrium. Bold arrows identify tangential forces arising from surface tension; thin arrows indicate the internal pressure forces acting on the cross-sectional area (shaded).

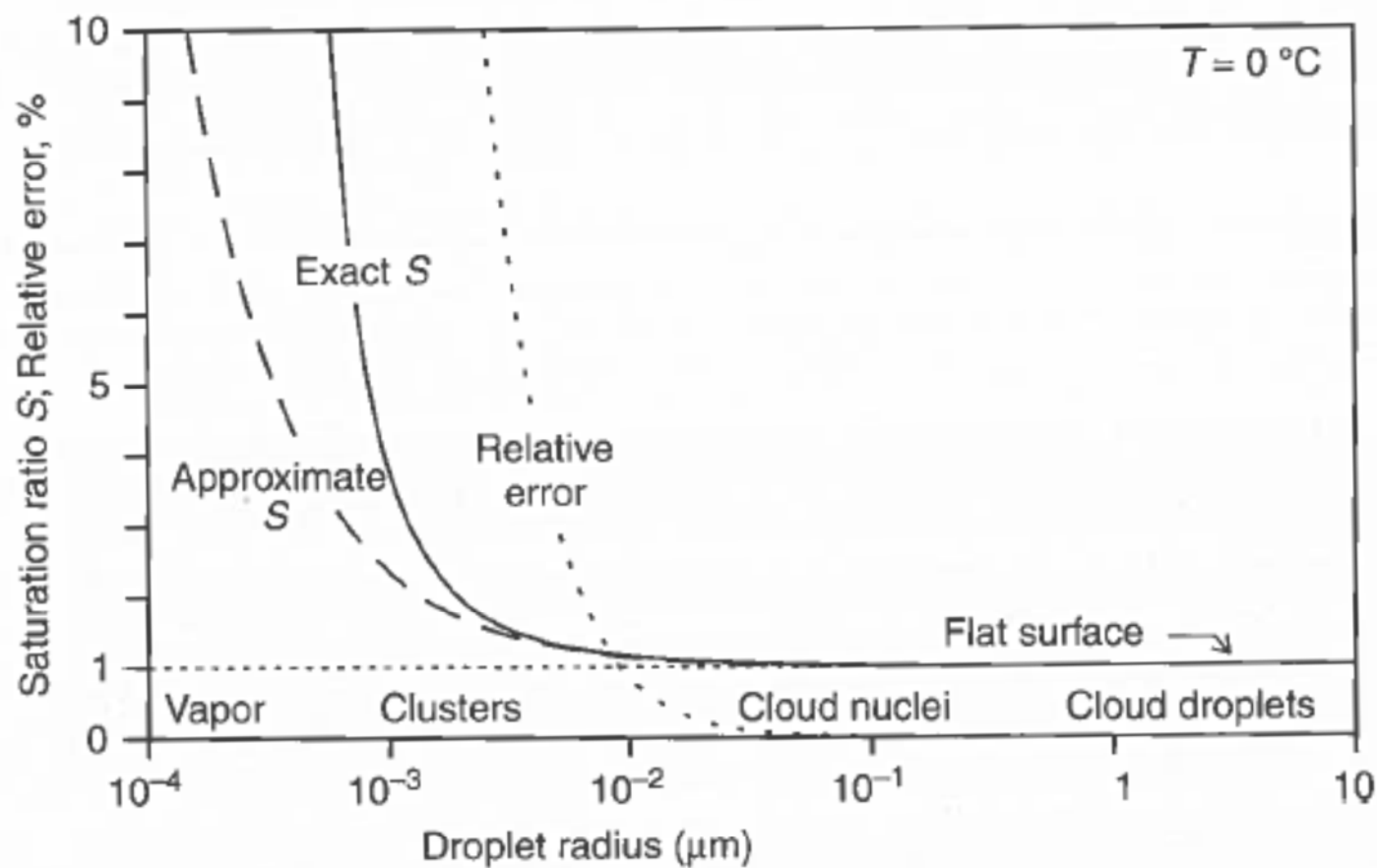


Figure 3.5 Exact and approximate dependences of saturation ratio S on droplet radius at temperature $T = 0^\circ\text{C}$.

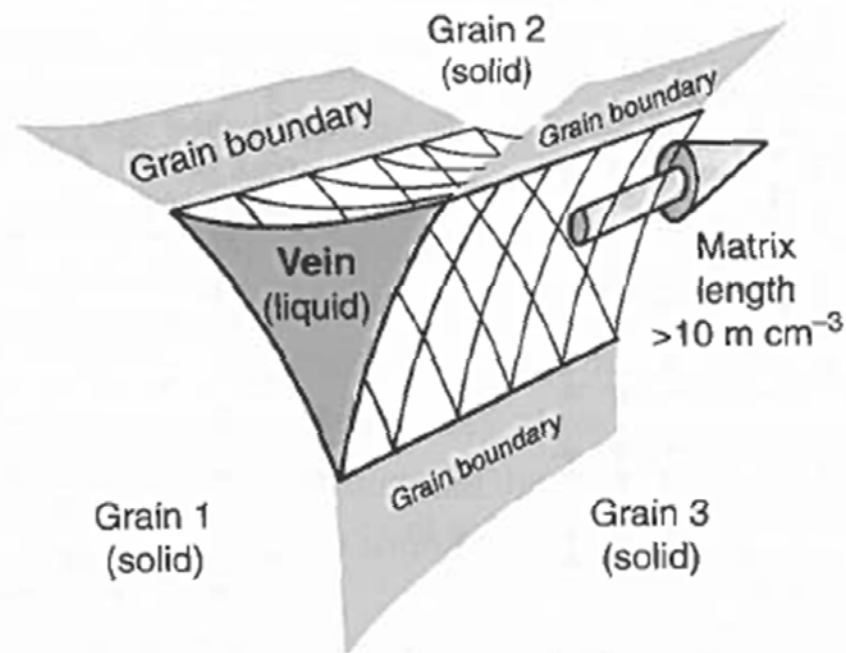


Figure 3.6 Perspective of grain boundaries at a triple junction in polycrystalline ice. Adapted from Mader (1992).

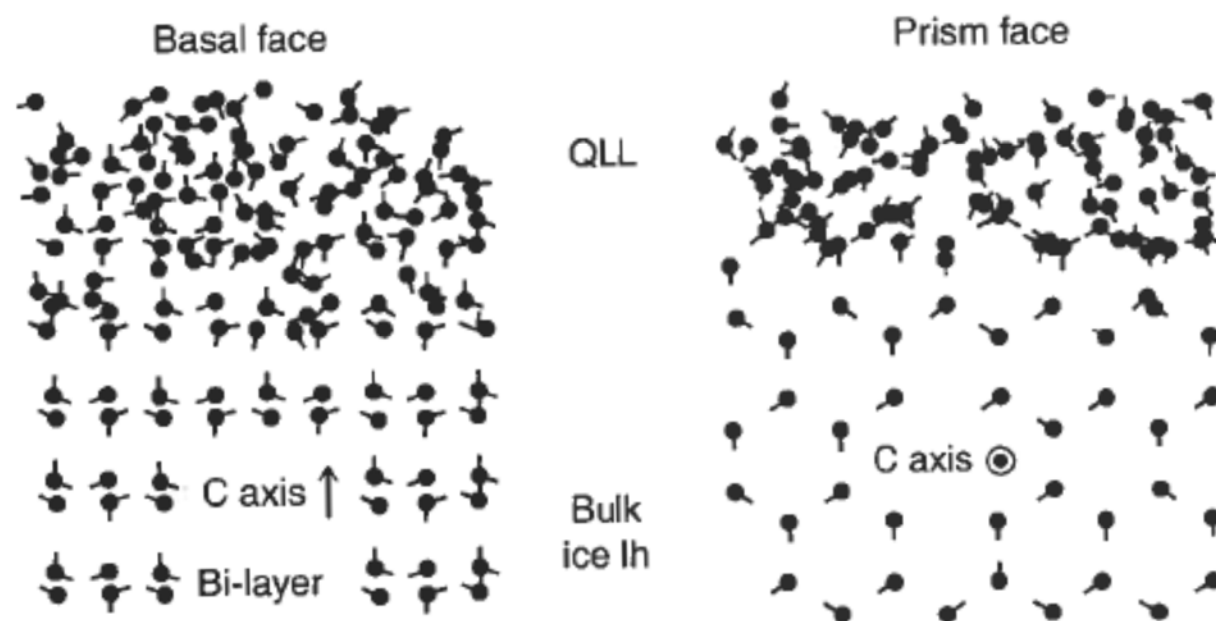


Figure 3.7 Results of molecular simulations of ice Ih showing molecular disorder at the solid–vapor interface. Left: Cross section parallel to the c axis (arrow up). Right: Cross section perpendicular to the c axis (arrow head on). Adapted with permission from Furukawa and Nada (1997). Copyright 1997 American Chemical Society.

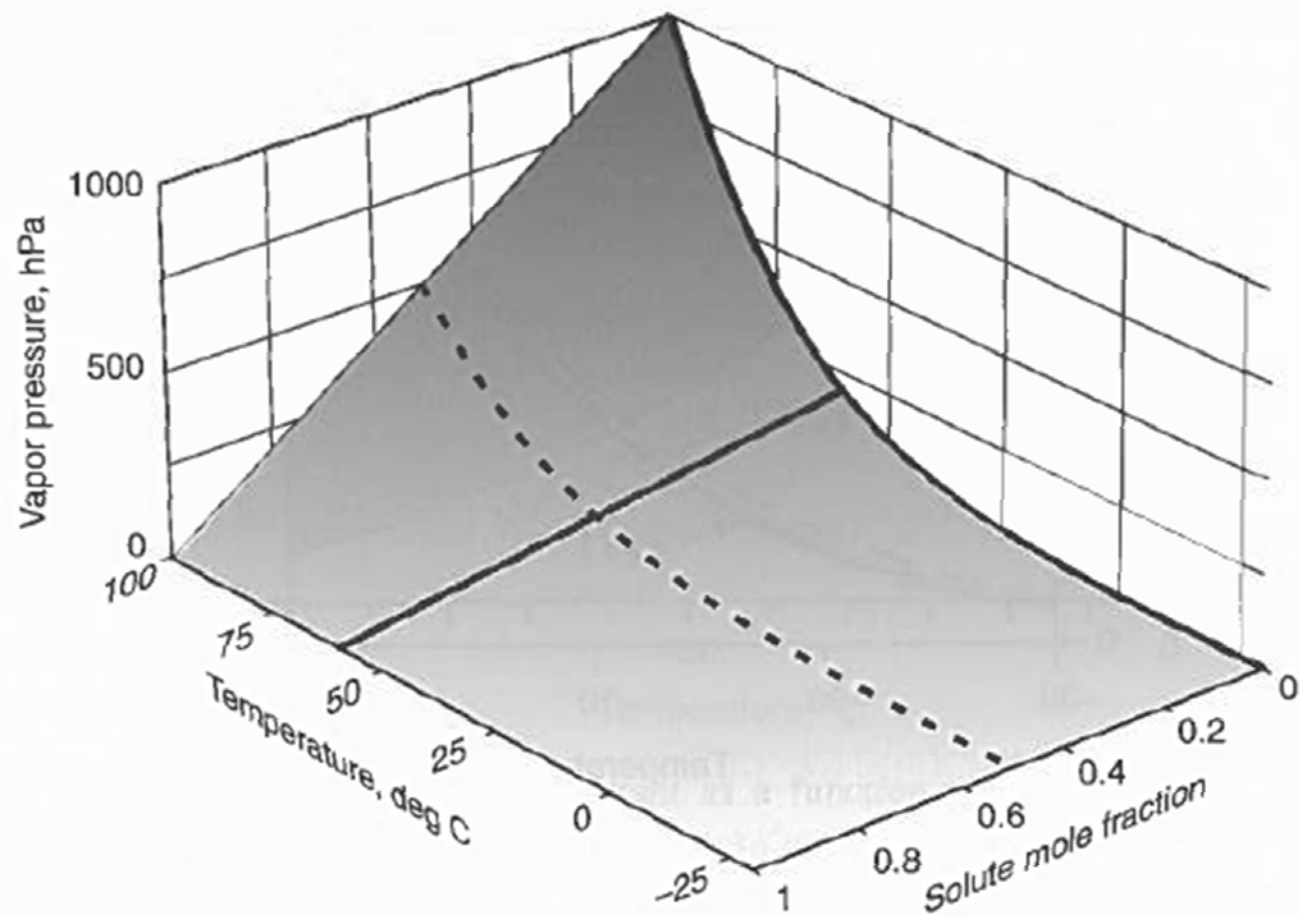


Figure 3.8 Effects of solute and temperature on the equilibrium vapor pressure of liquid water.

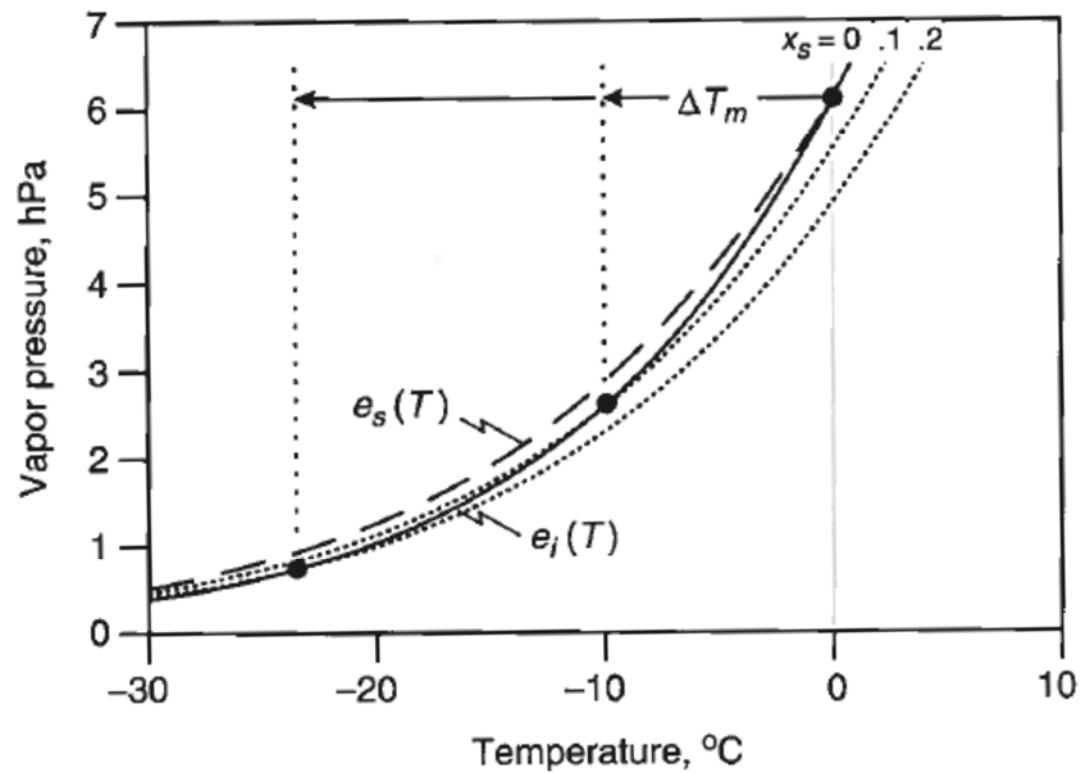


Figure 3.9 Concept behind the depression of the melting point of ice. The solute in solution lowers the equilibrium vapor pressure in proportion to the solute mole fraction x_s .

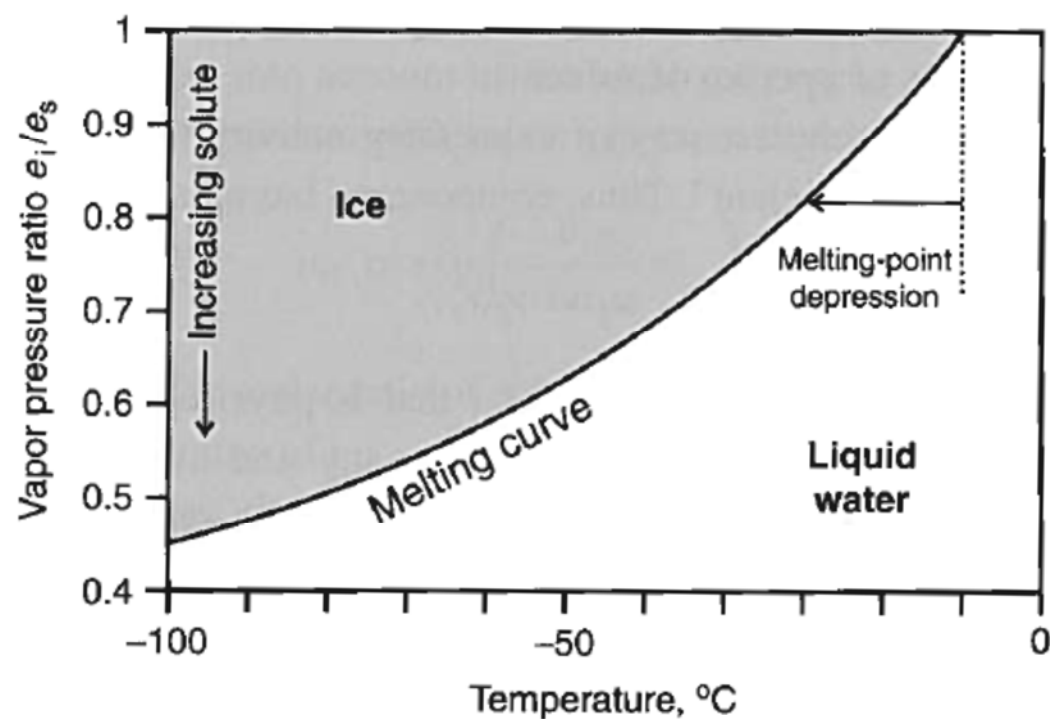


Figure 3.10 The depression of the melting point as a function of the activity of water. Solute concentration increases toward the right. Adapted from Koop *et al.* (2000).

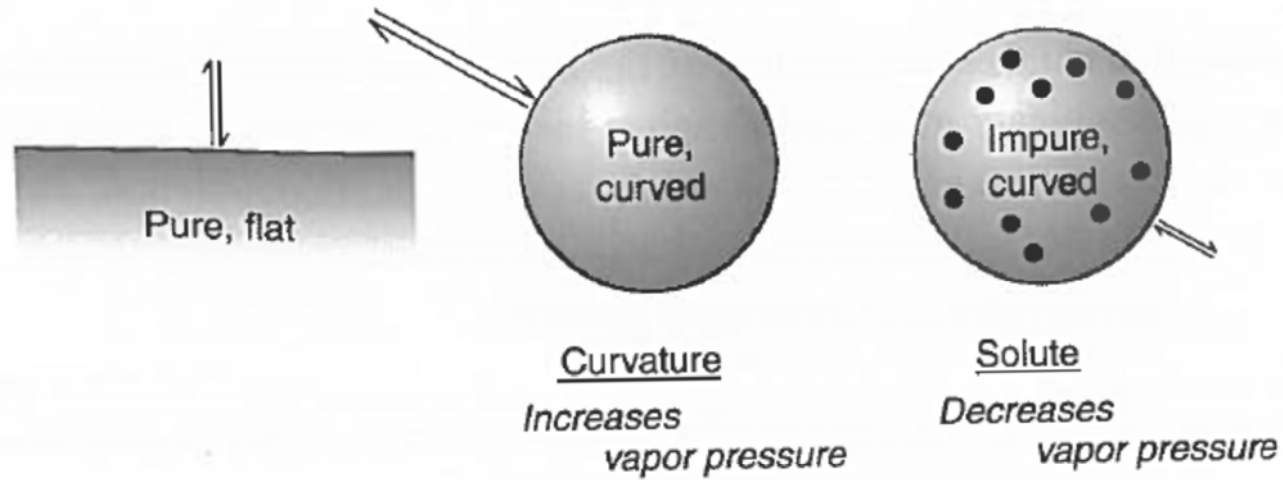


Figure 3.11 Illustration of the independent effects of curvature and solute on equilibrium vapor pressure.